From the Samuelson Volatility Effect to a Samuelson Correlation Effect: An Analysis of Crude Oil Calendar Spread Options

Lorenz SCHNEIDER[a], Bertrand TAVIN[a,*]

[a] *EMLYON Business School, Ecully, France*

Abstract

We introduce a multi-factor stochastic volatility model based on the CIR/Heston stochastic volatility process. In order to capture the Samuelson effect displayed by commodity futures contracts, we add expiry-dependent exponential damping factors to their volatility coefficients. The model leads to stochastic correlation between the returns of two futures contracts. The pricing of single underlying European options on futures contracts is straightforward and can incorporate the volatility smile or skew observed in the market. We calculate the joint characteristic function of two futures contracts in the model in analytic form and use it to price calendar spread options. We then propose analytical expressions to obtain the copula and copula density directly from the joint characteristic function of a pair of futures. These expressions are convenient to analyze the term-structure of dependence between the two futures produced by the model. In an empirical application we calibrate the model to volatility surfaces of vanilla options on WTI and provide evidence that the model is able to produce the desired stylized facts in terms of volatility and dependence. In particular, we observe that the returns of two futures are less dependent the greater the time-interval between their maturities is. In analogy to the classic Samuelson volatility effect, we call this effect the Samuelson correlation effect.

Keywords: Multi-factor stochastic volatility, Futures curve modelling, Option pricing, Crude oil, Fourier inversion methods

JEL: C02, G13

1. Introduction

Crude oil is by far the world's most actively traded commodity. It is usually traded on exchanges in the form of futures contracts. The two most important benchmark crudes are West Texas Intermediate (WTI), traded on the NYMEX, and Brent, traded on the ICE. In the S&P Goldman Sachs Commodity Index, WTI has a weight of 24.71% and Brent a weight of 22.34%, for a combined total of almost half the index. Another widely quoted index, Jim Rogers' RICI, has weights of 21% for WTI and 14% for Brent. The crude oil derivatives market is also the most liquid commodity derivatives market. Popular products are European, American, Asian, and calendar spread options on futures contracts.

*Corresponding author: EMLYON Business School, 23 Avenue Guy de Collongue, 69130 Ecully, France. Tel.: +33 (0)478337800 Fax: +33 (0)478336169.

Email addresses: schneider@em-lyon.com (Lorenz SCHNEIDER), tavin@em-lyon.com (Bertrand TAVIN)

An important empirical feature of crude oil markets is the absence of seasonality, which is in marked contrast to, say, agricultural commodities markets. A second empirical feature is stochastic volatility of futures contracts, which is clearly reflected in the oil volatility index (OVX), or "Oil VIX", introduced on the CBOE in July 2008. A third feature is known as the *Samuelson effect* (Samuelson, 1965; Bessembinder et al., 1996; Brooks, 2012), i.e. the empirical observation that a given futures contract increases in volatility as it approaches its maturity date. Finally, European and American options on futures tend to show a more or less strongly pronounced volatility smile, the shape of which depends on the option's maturity.

European and American options depend on the evolution of just one underlying futures contract. In contrast to these, calendar spread options have a payoff that is calculated from the difference of two futures contracts with different maturities. Therefore, a mathematical analysis and evaluation of calendar spread options must be carried out in a framework that models the joint stochastic behaviour of several futures contracts.

In this article, we propose a multi-factor stochastic volatility model for the crude oil futures curve. Like the popular Clewlow and Strickland (1999b,a) models, the model is futures-based, not spot-based, which means it can exactly match any given futures curve by accordingly specifying the futures' initial values without "using up" any of the other model parameters. The variance processes are based on the Cox et al. (1985) and Heston (1993) stochastic variance process. However, in order to capture the Samuelson effect, we add expiry dependent exponential damping factors. As in the Heston (1993) model, futures returns and variances are correlated, so that volatility smiles of American and European options observed in the market can be closely matched. The instantaneous correlation of the returns of two futures contracts is also stochastic in our multi-factor model, since it is calculated from the stochastic variances.

Our first result is the calculation of the joint characteristic function of the log-returns of two futures contracts in analytic form. Using this function, calendar spread option prices can be obtained via 1-dimensional Fourier integration as shown by Caldana and Fusai (2013) or the 2-dimensional Fast Fourier Transform (FFT) algorithm of Hurd and Zhou (2010). The fast speed of these algorithms is of great importance when calibrating the model to these products.

Our second result is to describe the dependence structure of two futures prices in terms of copulas obtained from the joint characteristic function of the model. In many studies, the measure chosen to describe dependence is Pearson's rho, which, however, depends on the marginal distributions. In our study, the use of copulas completely insulates our analysis from the influence of the marginals. Then, via the copula, dependence and concordance measures such as Spearman's rho and Kendall's tau are straightforward to compute.

Copula functions can also be used to give a rigorous definition of the implied correlation of calendar spread options. The traditional definition assumes a bivariate Black-Scholes-Merton model for the two underlyings, which assumes in particular that the marginal distributions are log-normal. In contrast, here, using the actual marginal distributions of the model, we consider the implied correlation for a given calendar spread

option price as the value of the correlation parameter in the bivariate Gaussian copula that reproduces this price.

In an empirical section we calibrate the two-factor version of our model to market data from three different dates. We show that the model can fit European and American option prices very closely. The model can therefore be used by a price maker in a crude oil market to provide consistent and arbitrage free prices to other market participants. Furthermore, we observe that, for a fixed time-horizon, the returns of two futures become less dependent as the maturity of the second underlying futures contract increases and moves away from that of the first underlying contract. In analogy to the classic Samuelson *volatility* effect, we call this effect the Samuelson *correlation* effect.

A detailed exposition of commodity models is given by Clark (2014). One of the most important and still widely used models is the Black (1976) futures model, which is set in the Black-Scholes-Merton framework. Contracts with different maturities can have different volatilities in this model, but for each contract the volatility is constant. Therefore, Black's model doesn't capture the Samuelson effect. Also, all contracts are perfectly correlated in this model, since they are driven by the same Brownian motion.

Clewlow and Strickland (1999b,a) propose one-factor and multi-factor models of the entire futures curve with deterministic time-dependent volatility functions. A popular specification for these functions is with exponential damping factors. Since this specification still leads to log-normally distributed futures prices, there is no volatility smile or skew in this model. In the one-factor model, the instantaneous returns of contracts with different maturities are perfectly correlated; in the multi-factor model, however, these returns are not perfectly, but deterministically correlated.

Stochastic volatility models have been proposed by Scott (1987, 1997), Hull and White (1987), Heston (1993), Bakshi et al. (1997) and Schoebel and Zhu (1999) among others. Christoffersen et al. (2009) study the stochastic correlation between the stock return and variance in a multi-factor version of the Heston (1993) model. Duffie et al. (2000) define a general class of jump-diffusions, into which the model presented in this paper fits. Trolle and Schwartz (2009) introduce a two-factor spot based model, with, in addition, two stochastic volatility factors as well as two stochastic factors for the forward cost-of-carry. The main focus of their study is on unspanned stochastic volatility of single-underlying options on futures contracts.

Spread options have been well studied in a two-factor Black-Scholes-Merton framework. Margrabe (1978) gives an exact formula when the strike K equals zero, and Kirk (1995), Carmona and Durrleman (2003), Bjerksund and Stensland (2011) and Venkatramanan and Alexander (2011) give approximation formulas for any K. Caldana and Fusai (2013) have recently proposed a very fast one-dimensional Fourier method that extends the approximation given by Bjerksund and Stensland (2011) to any model for which the joint characteristic function is known.

The rest of the paper proceeds as follows. In Section 2 we define the proposed model and provide the associated joint characteristic function. Section 3 deals with spread options and the structure of dependence produced by the model. Section 4 presents an empirical analysis based on different market situations. Section

5 concludes.

2. A Model with Stochastic Volatility for Crude Oil Futures

2.1. The Financial Framework and the Model

We begin by giving a mathematical description of our model under the risk-neutral measure $\mathbb{Q}$. Let $n \geq 1$ be an integer, and let $B_1, ..., B_{2n}$ be Brownian motions under $\mathbb{Q}$. Let T_m be the maturity of a given futures contract. The futures price $F(t, T_m)$ at time $t, 0 \leq t \leq T_m$, is assumed to follow the stochastic differential equation (SDE)

$$dF(t, T_m) = F(t, T_m) \sum_{j=1}^{n} e^{-\lambda_j (T_m - t)} \sqrt{v_j(t)} dB_j(t),\ F(0, T_m) = F_{m,0} > 0. \tag{1}$$

The processes $v_j, j = 1, ..., n$, are CIR/Heston square-root stochastic variance processes assumed to follow the SDE

$$dv_j(t) = \kappa_j \left(\theta_j - v_j(t)\right) dt + \sigma_j \sqrt{v_j(t)} dB_{n+j}(t),\ v_j(0) = v_{j,0} > 0. \tag{2}$$

For the correlations, we assume

$$\langle dB_j(t), dB_{n+j}(t) \rangle = \rho_j dt, -1 < \rho_j < 1, j = 1, ..., n, \tag{3}$$

and that otherwise the Brownian motions $B_j, B_k, k \neq j, j+n$, are independent of each other. As we will see, this assumption has as a consequence that the characteristic function factors into n separate expectations. For fixed T_m, the futures log-price $\ln F(t, T_m)$ follows the SDE

$$d \ln F(t, T_m) = \sum_{j=1}^{n} \left(e^{-\lambda_j (T_m - t)} \sqrt{v_j(t)} dB_j(t) - \frac{1}{2} e^{-2\lambda_j (T_m - t)} v_j(t) dt \right),\ \ln F(0, T_m) = \ln F_{m,0}. \tag{4}$$

Integrating (4) from time 0 up to a time $T, T \leq T_m$, gives

$$\ln F(T, T_m) - \ln F(0, T_m) = \sum_{j=1}^{n} \int_0^T e^{-\lambda_j (T_m - t)} \sqrt{v_j(t)} dB_j(t) - \frac{1}{2} \sum_{j=1}^{n} \int_0^T e^{-2\lambda_j (T_m - t)} v_j(t) dt. \tag{5}$$

We define the log-return between times 0 and T of a futures contract with maturity T_m as

$$X_m(T) := \ln \left(\frac{F(T, T_m)}{F(0, T_m)} \right).$$

In the following, the joint characteristic function ϕ of two log-returns $X_1(T), X_2(T)$ will play an important role. For $u = (u_1, u_2) \in \mathbb{C}^2$, ϕ is given by

$$\phi(u) = \phi(u; T, T_1, T_2) = \mathbb{E}^{\mathbb{Q}} \left[\exp \left(i \sum_{k=1}^{2} u_k X_k(T) \right) \right]. \tag{6}$$

The joint characteristic function Φ of the futures log-prices $\ln F(T, T_1), \ln F(T, T_2)$ is then given by

$$\Phi(u) = \exp \left(i \sum_{k=1}^{2} u_k \ln F(0, T_k) \right) \cdot \phi(u). \tag{7}$$

Note that futures prices in our model are not mean-reverting, and that the log-price $\ln F(t,T_m)$ at time t and the log-return $\ln F(T,T_m) - \ln F(t,T_m)$ are independent random variables. In the following proposition, we show how the joint characteristic function ϕ is given by a system of two ordinary differential equations (ODE).

Proposition 1. *The joint characteristic function ϕ at time $T \leq T_1, T_2$ for the log-returns $X_1(T), X_2(T)$ of two futures contracts with maturities T_1, T_2 is given by*

$$\begin{aligned}\phi(u) &= \phi(u;T,T_1,T_2)\\ &= \prod_{j=1}^{n} \exp\left(i\frac{\rho_j}{\sigma_j}\left\{\frac{\kappa_j\theta_j}{\lambda_j}(f_{j,1}(u,0) - f_{j,1}(u,T)) - f_{j,1}(u,0)v_j(0)\right\}\right)\exp\left(A_j(0,T)v_j(0) + B_j(0,T)\right),\end{aligned}$$

where

$$f_{j,1}(u,t) = \sum_{k=1}^{2} u_k e^{-\lambda_j(T_k - t)}, \quad f_{j,2}(u,t) = \sum_{k=1}^{2} u_k e^{-2\lambda_j(T_k - t)},$$
$$q_j(u,t) = i\rho_j\frac{\kappa_j - \lambda_j}{\sigma_j}f_{j,1}(u,t) - \frac{1}{2}(1-\rho_j^2)f_{j,1}^2(u,t) - \frac{1}{2}if_{j,2}(u,t),$$

and the functions $A_j : (t,T) \mapsto A_j(t,T)$ and $B_j : (t,T) \mapsto B_j(t,T)$ satisfy the two differential equations

$$\frac{\partial A_j}{\partial t} - \kappa_j A_j + \frac{1}{2}\sigma_j^2 A_j^2 + q_j = 0,$$
$$\frac{\partial B_j}{\partial t} + \kappa_j\theta_j A_j = 0,$$

with $A_j(T,T) = i\frac{\rho_j}{\sigma_j}f_{j,1}(u,T)$, $B_j(T,T) = 0$.

The single characteristic function ϕ_1 at time $T \leq T_1$ for the log-return $X_1(T)$ of a futures contract with maturity T_1 is given by setting $u_2 = 0$ in the joint characteristic function.

The statement regarding the single characteristic function immediately follows from the definition of the joint characteristic function. The joint characteristic function is calculated in Section 6.

In the next proposition, we show how this ODE system can be solved analytically. A closed form expression for A_j is found thanks to a computer algebra software and B_j is proportional to the integral of A_j on $[0,T]$.

Proposition 2. *Dropping the references to j, the function $A : (t,T) \mapsto A(t,T)$ is given in closed form as*

$$A(t,T) = \frac{1}{\sqrt{2}z\sigma}\cdot\frac{\left((M^-(t) - M^+(t))X_0 + X_1U^+(t)\right)C_1 - 2\left(M^+(t)X_0 - X_1U^+(t)\right)(C_3 - iC_2)e^{\lambda t}}{M^+(t)X_0 - X_1U^+(t)}$$
$$+ \frac{1}{\sigma^2}\cdot\frac{\left((\kappa-\lambda)M^+(t) + (\kappa+\lambda)M^-(t)\right)X_0 - \left((\kappa-\lambda)U^+(t) - 2\lambda U^-(t)\right)X_1}{M^+(t)X_0 - X_1U^+(t)},$$

with $z = \sqrt{C_2 + iC_3}$ and C_1, C_2, C_3 constants with respect to t, defined as

$$C_1 = \rho\frac{\kappa-\lambda}{\sigma}\sum_{k=1}^{2}u_k e^{-\lambda T_k}, \quad C_2 = -\frac{1}{2}(1-\rho^2)\left(\sum_{k=1}^{2}u_k e^{-\lambda T_k}\right)^2, \quad C_3 = -\frac{1}{2}\sum_{k=1}^{2}u_k e^{-2\lambda T_k},$$

$$
\begin{aligned}
X_0 &= 2YU^+(T) + 4z\lambda U^-(T),\\
X_1 &= 2YM^+(T) - 2\left(z(\lambda+\kappa) + \sigma\sqrt{2}\frac{C_1}{2}\right)M^-(T),\\
Y &= \sigma\sqrt{2}\left(\frac{C_1}{2} - ie^{\lambda T}C_2 + e^{\lambda T}C_3\right) - z\left(\kappa - \lambda - i\rho f_1(T)\sigma\right),
\end{aligned}
$$

$$
\begin{aligned}
M^{\pm}(t) &= M\left(\frac{\kappa z - \frac{\sigma\sqrt{2}}{2}C_1}{2z\lambda} \pm \frac{1}{2}, \frac{\kappa+\lambda}{\lambda}, \frac{\sigma\sqrt{2}}{\lambda}ize^{\lambda t}\right),\\
U^{\pm}(t) &= U\left(\frac{\kappa z - \frac{\sigma\sqrt{2}}{2}C_1}{2z\lambda} \pm \frac{1}{2}, \frac{\kappa+\lambda}{\lambda}, \frac{\sigma\sqrt{2}}{\lambda}ize^{\lambda t}\right).
\end{aligned}
$$

The functions M and U are the confluent hypergeometric functions.

A description of M and U functions as well as useful properties for their implementation can be found in Appendix A.

The models of Clewlow and Strickland (1999b,a) are useful benchmarks, so we give a description of them and calculate their joint characteristic function. In the risk-neutral measure $\mathbb{Q}$, the futures price $F(t,T_m)$ is modelled with deterministic time-dependent volatility functions $\hat{\sigma}_j(t,T_m)$:

$$
dF(t,T_m) = F(t,T_m)\sum_{j=1}^{n}\hat{\sigma}_j(t,T_m)dB_j(t), \tag{8}
$$

where $B_1,...,B_n$ are independent Brownian motions. A popular specification for the volatility functions is

$$
\hat{\sigma}_j(t,T_m) := e^{-\lambda_j(T_m-t)}\sigma_j \tag{9}
$$

for fixed parameters $\sigma_j, \lambda_j \geq 0$, so that the volatility of a contract a long time away from its maturity is damped by the exponential factor(s).

Proposition 3. *In the Clewlow and Strickland model defined by* (8) *and* (9)*, the joint characteristic function ϕ at time $T \leq T_1, T_2$ for the log-returns $X_1(T), X_2(T)$ of two futures contracts with maturities T_1, T_2 is given by*

$$
\begin{aligned}
\phi(u) &= \phi(u;T,T_1,T_2)\\
&= \prod_{j=1}^{n}\exp\left(-\frac{\sigma_j^2}{4\lambda_j}(e^{2\lambda_j T}-1)\left\{i(u_1e^{-2\lambda_j T_1} + u_2e^{-2\lambda_j T_2}) + (u_1e^{-\lambda_j T_1} + u_2e^{-\lambda_j T_2})^2\right\}\right).
\end{aligned}
$$

The single characteristic function ϕ_1 at time $T \leq T_1$ for the log-return of a futures contract with maturity T_1 is given by setting $u_2 = 0$ in the joint characteristic function.

We prove this result in Section 6.

This result can also be used to add non-stochastic volatility factors to the model by multiplying the joint characteristic function of Proposition 1 with one or more factors from Proposition 3. Since each "Clewlow-Strickland" factor depends on only two parameters λ_j and σ_j, it does not add a significant burden to the calibration to market data, while allowing for increased flexibility when fitting the model to the observed volatility term structure.

2.2. Pricing Vanilla Options

European options on futures contracts can be priced using the Fourier inversion technique as described in Heston (1993) and Bakshi and Madan (2000), or the FFT algorithm of Carr and Madan (1999). Alternatively, they can be priced by Monte Carlo simulation using discretizations of (1) (Euler scheme) or (4) (Log-Euler scheme) and of (2).

Let K denote the strike and T the maturity of a European call option on a futures contract F with maturity $T_m \geq T$, and let the single characteristic function Φ_1 of the futures log-price $\ln F(T, T_m)$ be given by $\Phi_1(u) = e^{iu \ln F(0,T_m)} \phi_1(u)$. In the general formulation of Bakshi and Madan (2000), the numbers

$$\Pi_1 := \frac{1}{2} + \frac{1}{\pi} \int_0^\infty \Re \left[\frac{e^{-iu \ln K} \Phi_1(u - i)}{iu \Phi_1(-i)} \right] du, \tag{10}$$

$$\Pi_2 := \frac{1}{2} + \frac{1}{\pi} \int_0^\infty \Re \left[\frac{e^{-iu \ln K} \Phi_1(u)}{iu} \right] du, \tag{11}$$

represent the probabilities of F finishing in-the-money at time T in case the futures F itself or a risk-free bond is used as numéraire, respectively. The price C of a European call option is then obtained with the formula $C = e^{-rT} \left(F(0, T_1) \Pi_1 - K \Pi_2 \right)$. European put options can be priced via put-call parity $C - P = e^{-rT} \left(F(0, T_1) - K \right)$.

American call and put options can be evaluated via Monte-Carlo simulation using the method of Longstaff and Schwartz (2001). Alternatively, the early exercise premium can be approximated with the formula of Barone-Adesi and Whaley (1987). Trolle and Schwartz (2009) address the issue of estimating European prices from American prices. Chockalingam and Muthuraman (2011) study the problem of pricing American options with stochastic volatility models, including the Heston model; quite possibly their method can be adapted to the model presented here.

A typical WTI volatility surface displays high implied volatilities at the short end and low implied volatilities at the long end. This is in line with the Samuelson effect. Furthermore, there is usually a strongly pronounced smile at the short end, and a weak smile at the long end.

3. Calendar Spread Options and Analysis of Dependence

In this section we review the pricing of calendar spread options and the notion of implied correlation. Then we introduce analytic results to obtain the copula function and its density from the joint characteristic function.

3.1. Calendar Spread Options written on WTI futures

Calendar spread options (CSO) are very popular options in commodities markets. There are two types of these options: calendar spread calls (CSC) and calendar spread puts (CSP). Like spread options in equities derivatives markets, their payoff depends on the price difference of two underlying assets. A call spread option on two equity shares S_1 and S_2 gives the holder, at time T, the payoff $\max \left(S_1(T) - S_2(T) - K, 0 \right)$, and a

put the payoff $\max\left(K-\left(S_1(T)-S_2(T)\right),0\right)$. In the case of calendar spread options, the two underlyings are two futures contracts on the same commodity, but with different maturities T_1 and T_2. Examples of CSOs are the NYMEX calendar spread options on WTI crude oil. A WTI CSC (CSP) represents an option to assume a long (short) position in the first expiring futures contract in the spread and a short (long) position in the second contract. There are also so-called *financial* CSOs traded on the NYMEX, which are cash settled. For pricing purposes we will not distinguish between these two settlement types in this paper. There is usually very good liquidity on 1-month spreads (for which $T_2 - T_1 = 1$ month), whereas options on $2, 3, 6$ and 12-month spreads are less liquid.

Let two futures maturities T_1, T_2, an option maturity T, and a strike K (which is allowed to be negative) be fixed. Then the payoffs of calendar spread call and put options, CSC and CSP, are respectively given by

$$CSC(T) = \left(F(T,T_1) - F(T,T_2) - K\right)^+, \tag{12}$$

$$CSP(T) = \left(K - \left(F(T,T_1) - F(T,T_2)\right)\right)^+. \tag{13}$$

To evaluate such options with a pricing model, the discounted expectation of the payoff must be calculated in the risk-neutral measure. Assuming a continuously-compounded risk-free interest rate r, we have at time $t_0 = 0$:

$$CSC(0,T,T_1,T_2,K) = e^{-rT}\mathbb{E}_0\left[\left(F(T,T_1) - F(T,T_2) - K\right)^+\right], \tag{14}$$

$$CSP(0,T,T_1,T_2,K) = e^{-rT}\mathbb{E}_0\left[\left(K - \left(F(T,T_1) - F(T,T_2)\right)\right)^+\right]. \tag{15}$$

Note that there is a model-independent put-call parity for calendar spread options:

$$CSC(0) - CSP(0) = e^{-rT}\left(F(0,T_1) - F(0,T_2) - K\right). \tag{16}$$

Apart from Monte-Carlo simulation (where simulation of the CIR/Heston process is well-understood), we are aware of three efficient methods to price spread options. The first two are suitable when the joint characteristic function is available. The third one is more direct but needs the marginals and joint distribution function of the underlying futures.

The formula of Bjerksund and Stensland (2011) for a joint Black-Scholes-Merton model is generalized by Caldana and Fusai (2013) to models for which the joint characteristic function is known. Strictly speaking, these methods give a lower bound for the spread option price. However, our tests lead us to agree with the above authors that this lower bound is very close to the actual price (typically the first three digits after the comma are the same), and we therefore regard this lower bound as the spread option's price itself. Furthermore, in case $K = 0$ the formula is exact (exchange option case). This method relies on a one-dimensional Fourier inversion and appears to be the most suitable to our model and setup. We give additional details on its implementation in Appendix B.

An alternative method that also works with the joint characteristic function of the log-returns has been proposed by Hurd and Zhou (2010). In their paper, the transform of the calendar spread payoff function

with a strike of $K = 1$ is calculated analytically, and the price of the corresponding option is then deduced from this result. This method needs a double integral to be evaluated numerically using the two-dimensional Fast Fourier Transform ($2d$ FFT).

Methods working with distribution functions instead of characteristic functions are also available to price calendar spread options. The most direct approach is to evaluate a double integral of the payoff function times the joint density of the two underlying futures contracts. However, we can write calendar spread option prices as *single* integrals over the marginal and joint distribution functions. The calendar spread call and put option prices are given, at $t = 0$ and for $K \geq 0$, by

$$CSC(0, K, T, T_1, T_2) = \int_0^{+\infty} \left(G_2(x, T, T_2) - G(x, x + K, T, T_1, T_2)\right) dx, \tag{17}$$

$$CSP(0, T, T_1, T_2, K) = \int_0^{+\infty} \left(G_1(x + K, T, T_1) - G(x, x + K, T, T_1, T_2)\right) dx, \tag{18}$$

where G_1 and G_2 are the marginal distribution functions of X_1 and X_2, respectively, and G is their joint distribution function. The case $K < 0$ is treated as a calendar spread option written on the reverse spread $F(T, T_2) - F(T, T_1)$ with the opposite strike $-K$.

In our model, the distribution functions involved in (17) and (18) are not readily available. However, it is possible to calculate G_1 and G_2 from the joint characteristic function ϕ of (X_1, X_2) using direct inversion formulas given by

$$G_1(x, T, T_1) = \frac{e^{ax}}{2\pi} \int_{-\infty}^{+\infty} e^{-iux} \frac{\phi(u + ia, 0, T, T_1, T_2)}{a - iu} du, \tag{19}$$

$$G_2(x, T, T_2) = \frac{e^{ax}}{2\pi} \int_{-\infty}^{+\infty} e^{-iux} \frac{\phi(0, u + ia, T, T_1, T_2)}{a - iu} du, \tag{20}$$

with a proper choice of the smoothing parameter $a > 0$. A detailed proof of these inversion results can be found in Le Courtois and Walter (2015). The joint distribution function G can be recovered in a similar way using a direct two-dimensional inversion formula.

Lemma 4.

$$G(x_1, x_2, T, T_1, T_2) = \frac{e^{a_1 x_1 + a_2 x_2}}{4\pi^2} \int_{-\infty}^{+\infty} \int_{-\infty}^{+\infty} e^{-i(u_1 x_1 + u_2 x_2)} \frac{\phi(u_1 + ia_1, u_2 + ia_2, T, T_1, T_2)}{(a_1 - iu_1)(a_2 - iu_2)} du_1 du_2. \tag{21}$$

The proof of this expression follows along the same lines as the one for the univariate case given by Le Courtois and Walter (2015). It is given in Section 6.

Inversion formulas (19),(20) and (21) are suitable for the use of FFT methods in one and two dimensions. We refer to Appendix D and Appendix E for more details about the implementation of these formulas.

For completeness, we note that the joint density $g(., T, T_1, T_2)$ of $X(T) = (X_1(T), X_2(T))$ is given by

$$g(x_1, x_2, T, T_1, T_2) = \frac{1}{4\pi^2} \int_{-\infty}^{+\infty} \int_{-\infty}^{+\infty} e^{-i(u_1 x_1 + u_2 x_2)} \phi(u_1, u_2, T, T_1, T_2) du_1 du_2. \tag{22}$$

The marginal densities $g_1(.,T,T_1)$ and $g_2(.,T,T_2)$ of $X_1(T)$ and $X_2(T)$, respectively, are recovered as

$$g_1(x_1,T,T_1) = \frac{1}{\pi}\int_0^{+\infty} \text{Re}\left[e^{-iux_1}\phi(u,0,T,T_1,T_2)\right] du, \tag{23}$$

$$g_2(x_2,T,T_2) = \frac{1}{\pi}\int_0^{+\infty} \text{Re}\left[e^{-iux_2}\phi(0,u,T,T_1,T_2)\right] du. \tag{24}$$

3.2. Implied Correlation for Calendar Spread Options

Given the price of a CSO, it is possible to extract an implied correlation reflecting the level of dependence embedded in the given price. This implied correlation can be defined as the parameter of the Gaussian copula that reproduces the observed price. It exists whenever the observed price is free of arbitrage. This copula-based definition has the advantage that it disentangles the impact of the marginals on the price of a CSO from the dependence structure.

For $\rho \in [-1,1]$, we denote by C_ρ^G the bivariate Gaussian copula with parameter ρ. Special cases are $C^G_{\rho=+1}(u_1,u_2) = C^+(u_1,u_2)$ and $C^G_{\rho=-1}(u_1,u_2) = C^-(u_1,u_2)$, for $(u_1,u_2) \in [0,1]^2$, where C^+ and C^- are the usual upper and lower Fréchet-Hoeffding bounds. For definitions and general theory about copula functions we refer to Nelsen (2006) and Mai and Scherer (2012).

When the chosen dependence structure is given by a Gaussian copula with correlation parameter ρ, and its marginals are G_1 and G_2, the price of the strike K calendar spread call option is denoted by CSC^G and is given by, for $\rho \in]-1,+1[$,

$$CSC^G(0,T,T_1,T_2,K,\rho) = e^{-rT}\int_0^{+\infty}\left(G_1(x,T) - C_\rho^G\left(G_1(x,T),G_2(x+K,T)\right)\right)dx, \tag{25}$$

and, for $\rho = \pm 1$

$$CSC^G(0,T,T_1,T_2,K,\rho=+1) = CSC_0^+(K) = e^{-rT}\int_0^1 \left(G_2^{-1}(u,T) - G_1^{-1}(u,T) - K\right)^+ du,$$

$$CSC^G(0,T,T_1,T_2,K,\rho=-1) = CSC_0^-(K) = e^{-rT}\int_0^1 \left(G_2^{-1}(u,T) - G_1^{-1}(1-u,T) - K\right)^+ du,$$

where CSC^+ and CSC^- denote the prices obtained for the calendar spread option when the chosen dependence structures are respectively C^+ and C^-.

The implied correlation ρ^* is now defined as the value of the correlation parameter in (25) that reproduces the observed market price. For a CSP, it is defined via put-call parity (16). One can easily show that for any arbitrage-free price, ρ^* exists and is unique. Note that implied correlation depends on both the strike and the maturity of the CSO. By analogy with implied volatility, these phenomena are referred to as implied correlation smile (or frown) and implied correlation term-structure.

3.3. Analysis of the Dependence Structure Between two Futures

We now turn to the analysis of the dependence between futures prices at a future time horizon in by our model. As we have seen, it is possible to recover the marginal and joint density and distribution functions from the joint characteristic function. Here we show how to obtain the copula function and its density.

Let $C(.,T)$ denote the copula function between the log-returns $X_1(T)$ and $X_2(T)$ of two futures contracts. Note that, expressed as a copula (or a copula density), the dependence between the log-returns is the same as the dependence between the prices themselves. For readability, we drop the explicit reference to T_1 and T_2 in the expressions in the remainder of the section.

Proposition 5. *The copula function C describing the dependence between $X_1(T)$ and $X_2(T)$ and the corresponding copula density c can be recovered, for $(v_1, v_2) \in [0,1]^2$, as*

$$C(v_1, v_2, T) = \frac{e^{a_1 G_1^{-1}(v_1,T) + a_2 G_2^{-1}(v_2,T)}}{4\pi^2} \cdot \int_{-\infty}^{+\infty} \int_{-\infty}^{+\infty} \frac{e^{-i(u_1 G_1^{-1}(v_1,T) + u_2 G_2^{-1}(v_2,T))} \phi(u_1 + ia_1, u_2 + ia_2, T)}{(a_1 - iu_1)(a_2 - iu_2)} du_1 du_2, \tag{26}$$

$$c(v_1, v_2, T) = \frac{\int_{-\infty}^{+\infty} \int_{-\infty}^{+\infty} e^{-i\left(u_1 G_1^{-1}(v_1,T) + u_2 G_2^{-1}(v_2,T)\right)} \phi(u_1, u_2, T) du_1 du_2}{\int_{-\infty}^{+\infty} e^{-iu G_1^{-1}(v_1,T)} \phi(u, 0, T) du \int_{-\infty}^{+\infty} e^{-iu G_2^{-1}(v_2,T)} \phi(0, u, T) du}, \tag{27}$$

where G_1^{-1} and G_2^{-1} are the inverse cumulative distribution functions of $X_1(T)$ and $X_2(T)$.

We prove this result in Section 6.

The dependence structure created by the model between $X_1(T)$ and $X_2(T)$ is entirely described by the copula function $C(.,T)$. This copula function depends on the chosen time horizon T, and we therefore have a term-structure of dependence that can be obtained from ϕ. The indexing by T of the copula C should be understood as a time-horizon, since it describes, seen from $t = 0$, the distribution of the random vector $(G_1(X_1(T), T), G_2(X_2(T), T))$. The chosen model produces a term-structure of dependence (i.e. a term-structure of copulas) which should not be confused with a time dependent copula.

Figure 1 plots the copula function and copula density between two futures prices obtained with the SV2F model and parameters as given in Table 1. The chosen futures respective maturities are $T_1 = 0.25$ years and $T_2 = 0.75$ years, and the chosen time horizon is $T = 0.25$ years.

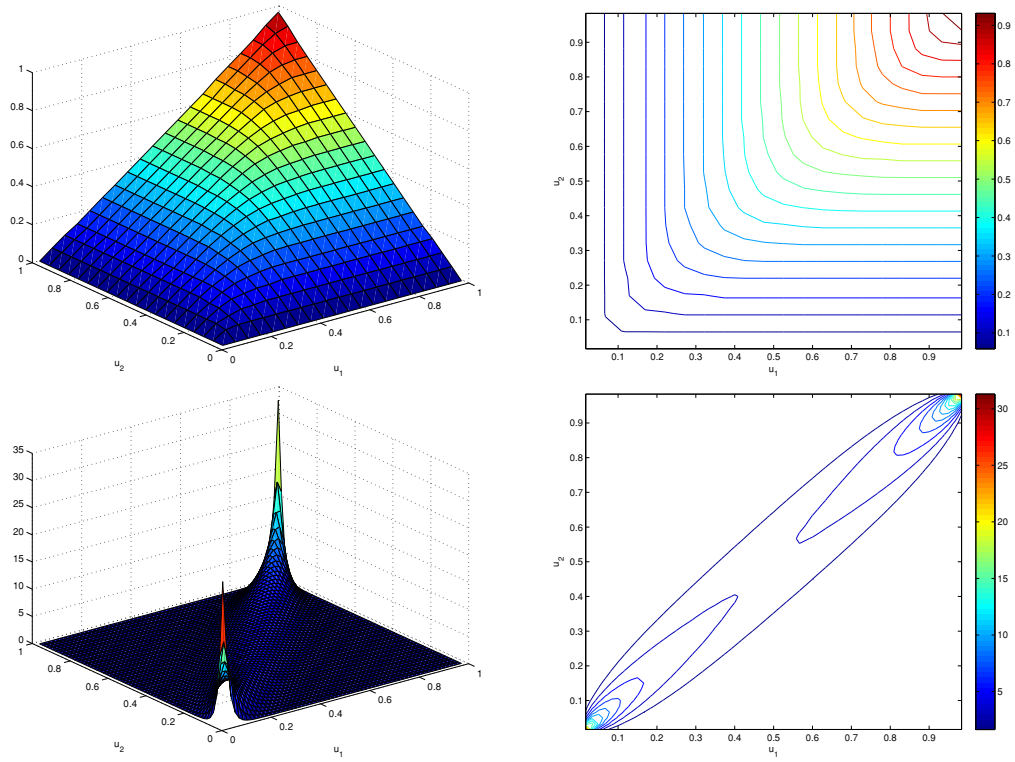

Figure 1: Copula function and copula density representing the dependence structure between $F(T, T_1)$ and $F(T, T_2)$, for $T = T_1 = 0.25$ years and $T_2 = 0.75$ years, obtained with SV2F model and parameters as given in Table 1.

κ_1	κ_2	θ_1	θ_2	ρ_1	ρ_2	σ_1	σ_2	$v_1(0)$	$v_2(0)$	λ_1	λ_2
1.00	1.00	0.16	0.09	0.00	0.00	0.25	0.20	0.16	0.09	0.10	2.00

Table 1: Model parameters used to illustrate the dependence structure between two futures in Section 3.3.

To assess the dependence between $X_1(T)$ and $X_2(T)$ with a single number instead of a function one can rely on concordance and dependence measures. Two well-known concordance measures are Kendall's tau and Spearman's rho. For $(X_1(T), X_2(T))$ these measures are denoted by $\tau_K(X_1, X_2, T)$ and $\varrho_S(X_1, X_2, T)$, respectively. Two well-known dependence measures are Schweizer-Wolf's sigma and Hoeffding's phi. For $(X_1(T), X_2(T))$ these measures are denoted by $\sigma_{SW}(X_1, X_2, T)$ and $\Phi_H(X_1, X_2, T)$, respectively. Concordance and dependence measures can be expressed as double integrals on the unit square $[0, 1]^2$ of the copula of $(X_1(T), X_2(T))$ and its density. We refer to Nelsen (2006) for statements of these expressions and properties of these measures.

4. Calibration to Market Data and Empirical Considerations

In this section we consider empirical data for WTI. We calibrate the two factor version of our model on different dates corresponding to different market situations. We then analyze the term-structure of

dependence produced by the calibrated model and the implied correlations obtained when pricing calendar spread options.

4.1. Data

We use three sets of WTI market data. Each data-set corresponds to a cross-section of futures and options closing prices on a given date. We have chosen three dates as representatives of different market situations. The first date is December 10, 2008; it reflects the financial crisis, as it was just months after the default of Lehman Brothers. Implied volatilities of short-maturity WTI vanilla options were above 80% and the OVX index rose above 90%. The second date is March 9, 2011 and corresponds to a market that is recovering from the deepest states of the crisis. The third date is April 9, 2014 that can be seen as a "*back to normal*" market situation, at least from the standpoint of market prices. Interest rates data and closing prices for futures as well as vanilla options were obtained from Bloomberg and Datastream.

4.2. Calibration to Vanilla Options

Models considered in this paper, namely SV2F (two-factor version of the proposed stochastic volatility model) and CS2F (two-factor version of the Clewlow-Strickland model), can be fitted to a cross-section of observed vanilla options prices. For each data-set we calibrate these models by minimizing the sum of squared errors between model and observed prices. For a given data-set, the calibrated model parameter set θ^* is obtained as

$$\theta^* = \arg\min_{\theta\in\Theta} \sum_{i=1}^{N_T}\sum_{j=1}^{N_K} \left(O(K_j,T_i,T_i;\theta) - O^{Obs}(K_j,T_i,T_i)\right)^2, \tag{28}$$

where Θ is the set of feasible model parameters, N_T the number of maturities in the options set, N_K the number of strikes for each maturity (without loss of generality we consider the same number of strikes to be available for each maturity). $O(.;\theta)$ denotes the option price obtained using the chosen model with parameter θ and $O^{Obs}(.)$ denotes the corresponding observed price. In the considered data-sets we work with five maturities, ranging from two months to four years (hence $N_T = 5$), and seven strikes for each maturity, that are specified in terms of moneyness with respect to the corresponding futures price. Specifically, these strikes are 60%, 80%, 90%, 100%, 110%, 120% and 150% (hence $N_K = 7$).

Once the minimization programs have been solved, the quality of the obtained calibration can be measured as mean absolute error (MAE) or root mean squared error (RMSE) on prices, which are calculated as

$$MAE = \sum_{i=1}^{N_T}\sum_{j=1}^{N_K} \frac{\left|O(K_j,T_i;\theta^*) - O^{Obs}(K_j,T_i)\right|}{N_K N_T},$$

$$RMSE = \sqrt{\sum_{i=1}^{N_T}\sum_{j=1}^{N_K} \frac{\left(O(K_j,T_i;\theta^*) - O^{Obs}(K_j,T_i)\right)^2}{N_K N_T}}.$$

Table 2 presents, for each data-set, these error measures obtained with the calibrated models. Due to the presence of implied volatility smiles along the strike-axis, the CS2F model is not able to closely match the

observed prices. In contrast, the SV2F model can provide a proper fit to both the strike-structure and the term-structure of implied volatilities. The error measures obtained with SV2F model appear to be around half a volatility point for MAE and around three quarters of a point for RMSE, which can be regarded as very good given the large strike and maturity spans of the option sets.

	MAE		MAE (ATM)		RMSE	
Date	Price	Vol.	Price	Vol.	Price	Vol.
CS2F Model						
Dec. 2008	0.4607	0.0156	0.5205	0.0148	0.5827	0.0180
Mar. 2011	0.5394	0.0169	0.3941	0.0082	0.6803	0.0243
Apr. 2014	0.2884	0.0162	0.2644	0.0074	0.3616	0.0226
SV2F Model						
Dec. 2008	0.1278	0.0052	0.1627	0.0062	0.1777	0.0066
Mar. 2011	0.2071	0.0056	0.2419	0.0056	0.2922	0.0078
Apr. 2014	0.1113	0.0043	0.0965	0.0026	0.1517	0.0059

Table 2: MAE and RMSE error measures, of prices and implied volatilities, for SV2F and CS2F models calibrated to vanilla option prices. *Left panel* is for MAE on the whole matrix of options, *central panel* is for MAE on at-the-money options and *right panel* is for RMSE on the whole matrix of options.

4.3. Results

Figure 2 plots, for each data-set, implied volatility corresponding to the market data and implied volatility obtained with the SV2F model calibrated to vanilla option prices. Plots in the left column give evidence of the implied volatility smile in our data-sets. It can also be noted that the convexity and skew (at-the-money slope) of these smiles vary with maturity. This maturity effect is particularly present in the March 2011 data. Plots in the right column represent at-the-money volatility term-structure. They provide evidence for the empirical Samuelson volatility effect in the market prices of at-the-money vanilla options. Figure 2 shows that our model, once calibrated to vanilla option prices, is able to properly reproduce the empirical stylized facts for implied volatility, namely presence and maturity-dependency of the smile and Samuelson effect.

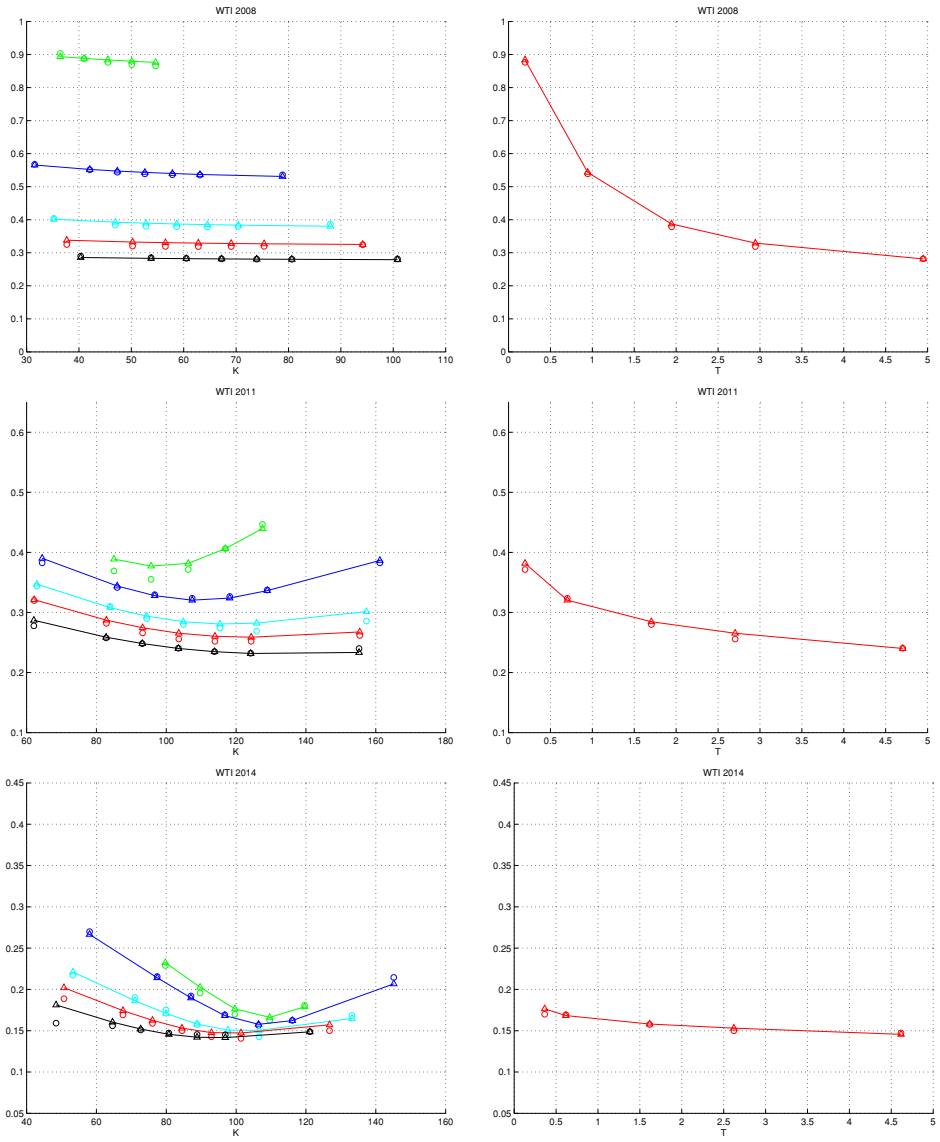

Figure 2: Implied volatilities corresponding to market quotes and obtained with SV2F model calibrated to vanilla options. *Left column*: implied volatility smiles. *Right column*: at-the-money implied volatility term-structure.

Figure 3 plots, for the data-sets of December 2008 and March 2011, measures of concordance and dependence between two futures prices produced by the calibrated SV2F model. This figure represents a type of dependence term-structure that is of interest for WTI futures market participants. It corresponds to the case where the time horizon and the first futures expiry are both held constant, while the difference between futures expiries varies. We observe that, as the difference between expiries increases, the pair of futures becomes less dependent which is in line with the intuition one can have *a priori*. We call this phenomenon the *Samuelson correlation effect*. This phenomenon is a desirable feature for a model to be used by a price maker quoting and trading a range of products written on WTI. The presented empirical applications show it is properly reproduced by the proposed model.

Figure 4 plots, for the data-sets of December 2008 and March 2011, measures of concordance and depen-

dence between two futures prices produced by the calibrated SV2F model. It corresponds to the case where the time horizon varies while the difference between futures expiries is held constant. For the December 2008 case, the level of dependence between the futures is little affected by the time-horizon. For the March 2011 case, as the time-horizon increases, the pairs of futures with 6-month difference between their maturities become more dependent. Here the intuition does not lead to a particular structure that is desirable, namely increasing or decreasing as the time horizon varies.

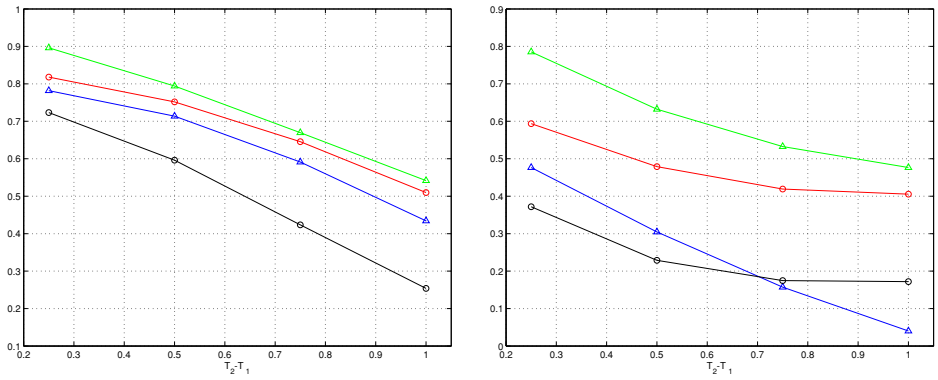

Figure 3: Term-structure of concordance and dependence measures between $F(T,T_1)$ and $F(T,T_2)$ produced by the SV2F model calibrated market data. *Left panel* corresponds to December 2008 data and *right panel* corresponds to March 2011 data. Time horizon T and first futures expiry T_1 are fixed at 3 months, T_2-T_1 ranges from 3 months to 1 year. Dependence measures are τ_K and ϱ_S (respectively, *green* and *blue* lines). Concordance measures are σ_{SW} and Φ_H (respectively, *red* and *black* lines).

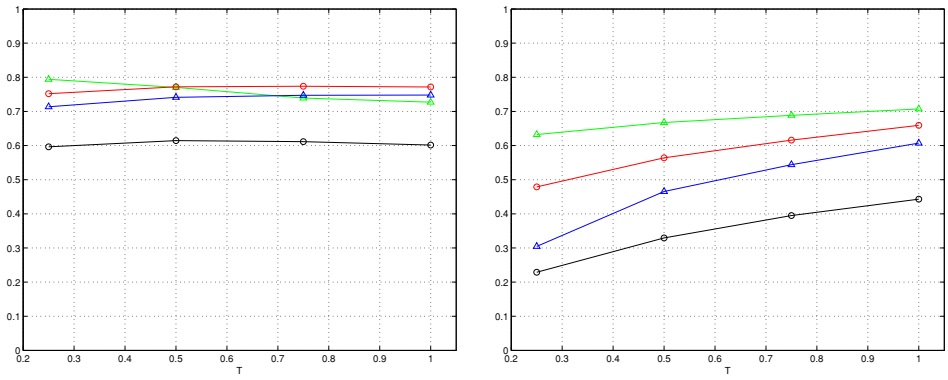

Figure 4: Term-structure of concordance and dependence measures between $F(T,T_1)$ and $F(T,T_2)$ produced by the SV2F model calibrated market data. *Left panel* corresponds to December 2008 data and *right panel* corresponds to March 2011 data. Time horizon T and first futures expiry T_1 range from 3 months to 1 year. T_2-T_1 is held fixed at 6 months. Dependence measures are τ_K and ϱ_S (respectively, *green* and *blue* lines). Concordance measures are σ_{SW} and Φ_H (respectively, *red* and *black* lines).

Figure 5 plots the implied correlation strike and maturity structures from spread option prices obtained with the SV2F model calibrated to the data-sets of December 2008 and March 2011. The considered spread options have fixed maturity and first futures expiry, while the difference between the two underlying futures expiries varies. For each pair of underlying futures, the five strikes correspond to a set of shifts applied to the

at-the-money spread $F(0,T_1) - F(0,T_2)$. These shifts are $-10, -5, -2.5, 0, +2.5, +5$ and $+10$. We observe that the obtained term-structures are decreasing. This observation is in line with the intuition and with what is observed in Figure 3, i.e. with the *Samuelson correlation effect*. For the March 2011 case, the model produces a non-constant strike structure of implied correlation. We observe that for larger strikes (out-of-the-money call spread options) implied correlations are lower than at-the-money. Lower implied correlations in turn correspond to higher option prices. For the December 2008 case, the model produces a rather flat strike structure of implied correlation. Hence, in this case, the prices produced by the model are close to prices that could have been produced using Gaussian copulas for the dependence between futures prices.

Figure 6 plots the implied correlation strike and maturity structures from spread option prices obtained with the SV2F model calibrated to the data-sets of December 2008 and March 2011. The considered spread options have maturity and first futures expiry that vary, while the difference between the two underlying futures expiries is held constant. For each pair of underlying futures, the five strikes correspond to a set of shifts applied to the at-the-money spread $F(0,T_1) - F(0,T_2)$. These shifts are the same as for Figure 5. We observe that the obtained term-structures are decreasing. The obtained term-structure for December 2008 is rather flat which is consistent with the term-structure of concordance and dependence presented in Figure 4. For the March 2011 case, the implied correlation term-structure is increasing which is again consistent with concordance and dependence measures in Figure 4. For the March 2011 case, the model produces a non-constant strike structure of implied correlation. For the December 2008 case, the model produces a rather flat strike structure of implied correlation. These strike structures are similar to those found in Figure 5 and the same comments apply.

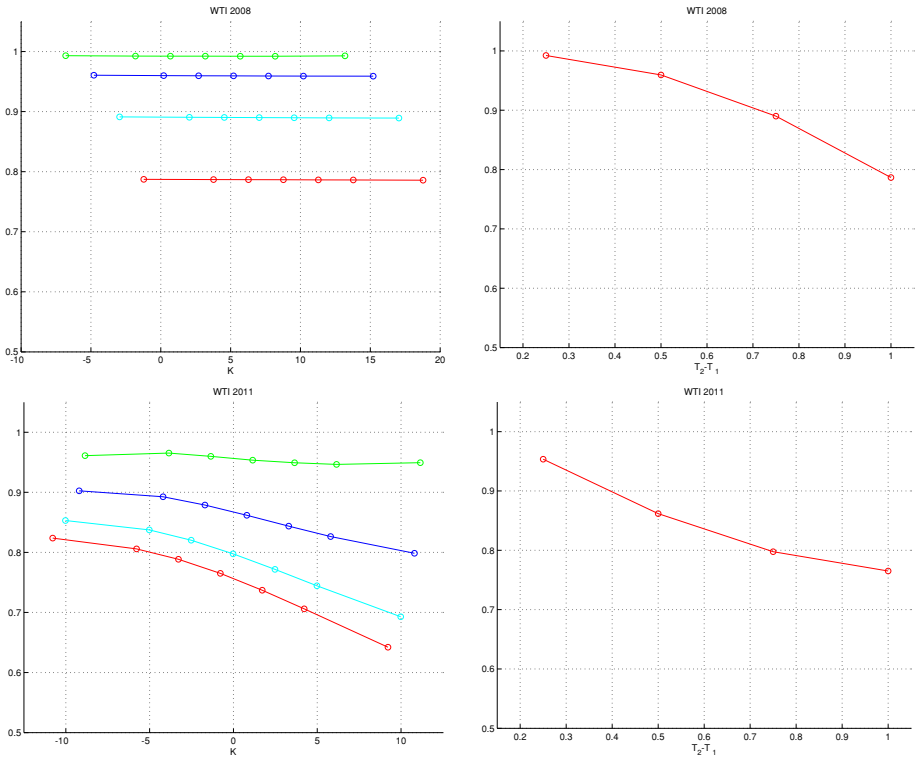

Figure 5: Implied correlations from spread option prices obtained with the SV2F model calibrated to market data of December 2008 and March 2011. The considered spread options have a maturity T and first underlying futures expiry T_1 fixed at 3 months. $T_2 - T_1$, the difference between the underlying futures expiries, ranges from 3 months to 1 year. *Left column*: implied correlation smiles. *Right column*: at-the-money implied correlation term-structure.

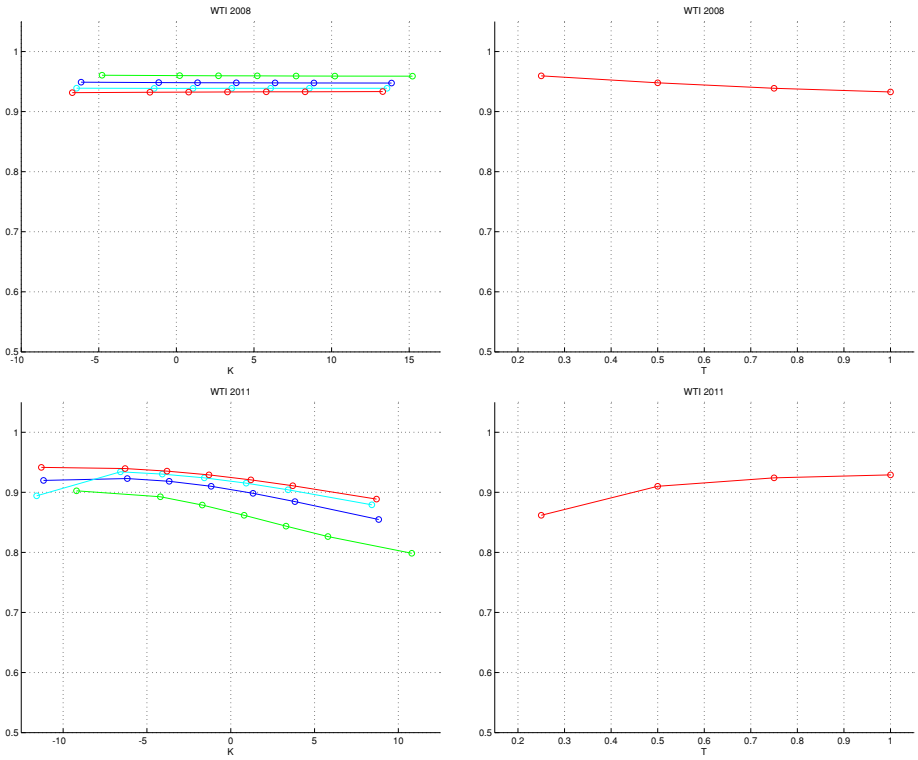

Figure 6: Implied correlations from spread option prices obtained with the SV2F model calibrated to market data of December 2008 and March 2011. The considered spread options have a maturity T and first underlying futures expiry T_1 varying from 3 months to 1 year. $T_2 - T_1$, the difference between the underlying futures expiries, is held fixed at 6 months. *Left column*: implied correlation smiles. *Right column*: at-the-money implied correlation term-structure.

5. Conclusion

We propose a multi-factor stochastic volatility model for commodity futures contracts. In order to capture the Samuelson effect displayed by commodity futures contracts, we add expiry-dependent exponential damping factors to their volatility coefficients. The pricing of single underlying European options on futures contracts is straightforward and can incorporate the volatility smile or skew observed in the market. We calculate the joint characteristic function of two futures contracts in the model and use the one-dimensional Fourier inversion method of Caldana and Fusai (2013) to price calendar spread options. Furthermore, we analyze the term-structure of dependence between pairs of futures in the model. We do this by showing how to obtain the copula and copula density functions directly from the joint characteristic function. When calibrated to vanilla options, the model is found to be able to produce stylized facts such as Samuelson effect and implied volatility smile as well as a decreasing term-structure of dependence and implied correlation smile for spread options.

6. Proofs

Proof. (Proposition 1)

We have

$$\begin{aligned}\phi(u) = \phi(u;T,T_1,T_2) &= \mathbb{E}\left[\exp\left(i\sum_{k=1}^{2} u_k X_k(T)\right)\right] \\ &= \mathbb{E}\left[\exp\left(i\sum_{k=1}^{2} u_k \left\{\sum_{j=1}^{n}\int_0^T e^{-\lambda_j(T_k-t)}\sqrt{v_j(t)}dB_j(t) - \frac{1}{2}\sum_{j=1}^{n}\int_0^T e^{-2\lambda_j(T_k-t)}v_j(t)dt\right\}\right)\right] \\ &= \prod_{j=1}^{n} E_j(u,T),\end{aligned}$$

where E_j is a function of u and T given by

$$E_j(u,T) = \mathbb{E}\left[\exp\left(i\sum_{k=1}^{2} u_k \left\{\int_0^T e^{-\lambda_j(T_k-t)}\sqrt{v_j(t)}dB_j(t) - \frac{1}{2}\int_0^T e^{-2\lambda_j(T_k-t)}v_j(t)dt\right\}\right)\right]$$

that otherwise depends only on the j-th model parameters $\lambda_j, \kappa_j, \theta_j, \sigma_j, v_{j,0}, \rho_j$.

We now calculate the function E_j. Since we are considering a fixed value of j, we drop this subscript in the following calculations. We also write $\tilde{B}$ for B_{n+j}, the Brownian motion driving the j-th variance process. Then we can decompose $B = B_j$, whose correlation with $\tilde{B} = B_{n+j}$ is given in equation (3) by $\langle B_j, B_{n+j}\rangle = \rho_j dt = \rho dt$, as $B = \rho\tilde{B} + \sqrt{1-\rho^2}\hat{B}$, where $\hat{B}$ is uncorrelated with $\tilde{B}$. Define the functions f_1, f_2 and q given by

$$\begin{aligned} f_1(u,t) &= \sum_{k=1}^{2} u_k e^{-\lambda(T_k-t)}, \quad f_2(u,t) = \sum_{k=1}^{2} u_k e^{-2\lambda(T_k-t)}, \\ q(u,t) &= i\rho\frac{\kappa-\lambda}{\sigma}f_1(u,t) - \frac{1}{2}(1-\rho^2)f_1^2(u,t) - \frac{1}{2}if_2(u,t).\end{aligned}$$

For simplicity, we write $f_1(t)$ for $f_1(u,t), f_2(t)$ for $f_2(u,t)$ and $q(t)$ for $q(u,t)$ in the following.

We first need an auxiliary result in order to calculate the characteristic function.

Lemma 6.

$$\sigma\int_0^T f_1(t)\sqrt{v(t)}d\tilde{B}(t) = \left[f_1(t)\left\{v(t) - \frac{\kappa\theta}{\lambda}\right\}\right]_0^T + (\kappa-\lambda)\int_0^T f_1(t)v(t)dt. \tag{29}$$

Proof. (Lemma 6)

Multiplying equation (2) by $f_1(t)$ and then integrating from 0 to T gives

$$\int_0^T f_1(t)dv(t) = \int_0^T f_1(t)\kappa(\theta - v(t))dt + \sigma\int_0^T f_1(t)\sqrt{v(t)}d\tilde{B}(t). \tag{30}$$

Using Itô-integration by parts (see Øksendal (2003)), we also have

$$\int_0^T f_1(t)dv(t) = [f_1(t)v(t)]_0^T - \int_0^T v(t)df_1(t) = [f_1(t)v(t)]_0^T - \lambda\int_0^T f_1(t)v(t)dt. \tag{31}$$

Equating the right hand sides of equations (30) and (31) gives

$$\begin{aligned}\sigma\int_0^T f_1(t)\sqrt{v(t)}d\tilde{B}(t) &= [f_1(t)v(t)]_0^T - \lambda\int_0^T f_1(t)v(t)dt - \int_0^T f_1(t)\kappa(\theta - v(t))dt \\ &= [f_1(t)v(t)]_0^T - \kappa\theta\int_0^T f_1(t)dt + (\kappa-\lambda)\int_0^T f_1(t)v(t)dt \\ &= \left[f_1(t)\left\{v(t) - \frac{\kappa\theta}{\lambda}\right\}\right]_0^T + (\kappa-\lambda)\int_0^T f_1(t)v(t)dt,\end{aligned}$$

which proves the lemma. □

We now calculate $E(u,T)$.

$$\begin{aligned}E(u,T) &= \left[\exp\left(i\sum_{k=1}^2 u_k\left\{\int_0^T e^{-\lambda(T_k-t)}\sqrt{v(t)}dB(t) - \frac{1}{2}\int_0^T e^{-2\lambda(T_k-t)}v(t)dt\right\}\right)\right] \\ &= \mathbb{E}\left[\exp\left(i\int_0^T f_1(t)\sqrt{v(t)}dB(t) - \frac{1}{2}i\int_0^T f_2(t)v(t)dt\right)\right] \\ &= \mathbb{E}\left[\exp\left(i\rho\int_0^T f_1(t)\sqrt{v(t)}d\tilde{B}(t) + i\sqrt{1-\rho^2}\int_0^T f_1(t)\sqrt{v(t)}d\hat{B}(t) - \frac{1}{2}i\int_0^T f_2(t)v(t)dt\right)\right] \\ &= \mathbb{E}\left[\exp\left(i\rho\int_0^T f_1(t)\sqrt{v(t)}d\tilde{B}(t) - \frac{1}{2}(1-\rho^2)\int_0^T (f_1(t))^2 v(t)dt - \frac{1}{2}i\int_0^T f_2(t)v(t)dt\right)\right] \\ &= \mathbb{E}\Big[\exp\Big(i\frac{\rho}{\sigma}\left[f_1(t)\left\{v(t) - \frac{\kappa\theta}{\lambda}\right\}\right]_0^T + i\rho\frac{\kappa-\lambda}{\sigma}\int_0^T f_1(t)v(t)dt \\ &\quad - \frac{1}{2}(1-\rho^2)\int_0^T (f_1(t))^2 v(t)dt - \frac{1}{2}i\int_0^T f_2(t)v(t)dt\Big)\Big] \\ &= \exp\left(i\frac{\rho}{\sigma}\left\{\frac{\kappa\theta}{\lambda}(f_1(0) - f_1(T)) - f_1(0)v(0)\right\}\right)\cdot\mathbb{E}\left[\exp\left(i\frac{\rho}{\sigma}f_1(T)v(T) + \int_0^T q(t)v(t)dt\right)\right].\end{aligned}$$

The expectation in the last line can be computed using the Feynman-Kac theorem (see Øksendal (2003)). Define the function h given by

$$h(t,v) = \mathbb{E}\left[\exp\left(i\frac{\rho}{\sigma}f_1(T)v(T) + \int_t^T q(s)v(s)ds\right)\right].$$

Then h satisfies the PDE

$$\frac{\partial h}{\partial t}(t,v) + \kappa(\theta - v(t))\frac{\partial h}{\partial v}(t,v) + \frac{1}{2}\sigma^2 v(t)\frac{\partial^2 h}{\partial v^2}(t,v) + q(t)v(t)h(t,v) = 0, \tag{32}$$

with terminal condition $h(T,v) = \exp\left(i\frac{\rho}{\sigma}f_1(T)v(T)\right)$. We know from Duffie et al. (2000) that h has affine form

$$h(t,v) = \exp\left(A(t,T)v(t) + B(t,T)\right), \tag{33}$$

with $A(T,T) = i\frac{\rho}{\sigma}f_1(T), B(T,T) = 0$. Putting (33) in (32) gives

$$B_t + A_t v + \kappa(\theta - v)A + \frac{1}{2}\sigma^2 v A^2 + qv = 0,$$

and collecting the terms with and without v leads to the two ODEs

$$A_t - \kappa A + \frac{1}{2}\sigma^2 A^2 + q = 0, \tag{34}$$

$$B_t + \kappa\theta A = 0. \tag{35}$$

This completes the proof of the proposition. □

Proof. (Proposition 3)

We calculate the joint characteristic function in the Clewlow and Strickland (1999a) model as follows.

$$\begin{aligned}
\phi(u) &= \phi(u; T, T_1, T_2) \\
&= \mathbb{E}\left[\exp\left(i\sum_{k=1}^{2} u_k X_k(T)\right)\right] \\
&= \mathbb{E}\left[\exp\left(i\sum_{k=1}^{2} u_k \left\{\sum_{j=1}^{n}\int_0^T e^{-\lambda_j(T_k-t)}\sigma_j dB_j(t) - \frac{1}{2}\sum_{j=1}^{n}\int_0^T e^{-2\lambda_j(T_k-t)}\sigma_j^2 dt\right\}\right)\right] \\
&= \prod_{j=1}^{n}\mathbb{E}\left[\exp\left(i\sum_{k=1}^{2} u_k \left\{\int_0^T e^{-\lambda_j(T_k-t)}\sigma_j dB_j(t) - \frac{1}{2}\int_0^T e^{-2\lambda_j(T_k-t)}\sigma_j^2 dt\right\}\right)\right] \\
&= \prod_{j=1}^{n}\exp\left(i\sum_{k=1}^{2} u_k \left\{-\frac{1}{2}\int_0^T e^{-2\lambda_j(T_k-t)}\sigma_j^2 dt\right\}\right)\mathbb{E}\left[\exp\left(i\sum_{k=1}^{2} u_k \left\{\int_0^T e^{-\lambda_j(T_k-t)}\sigma_j dB_j(t)\right\}\right)\right] \\
&= \prod_{j=1}^{n}\exp\left(i\sum_{k=1}^{2} u_k \left[-\frac{\sigma_j^2}{4\lambda_j}e^{-2\lambda_j(T_k-t)}\right]_0^T\right)\exp\left(-\frac{\sigma_j^2}{4\lambda_j}\left[\left(\sum_{k=1}^{2} u_k e^{-\lambda_j(T_k-t)}\right)^2\right]_0^T\right) \\
&= \prod_{j=1}^{n}\exp\left(-\frac{\sigma_j^2}{4\lambda_j}(e^{2\lambda_j T}-1)\left\{i(u_1 e^{-2\lambda_j T_1} + u_2 e^{-2\lambda_j T_2}) + (u_1 e^{-\lambda_j T_1} + u_2 e^{-\lambda_j T_2})^2\right\}\right).
\end{aligned}$$

This completes the proof of the proposition. □

Proof. (Lemma 4)

The proof to obtain this expression is the same, *mutatis mutandis*, as the proof in the univariate case provided in Le Courtois and Walter (2015). For ease of reading, we drop the explicit dependencies on T, T_1 and T_2. Let $a_1 > 0$ and $a_2 > 0$ be fixed and h be the function defined by

$$h(x_1, x_2) = e^{-(a_1 x_1 + a_2 x_2)}G(x_1, x_2) = e^{-(a_1 x_1 + a_2 x_2)}\int_{-\infty}^{x_2}\int_{-\infty}^{x_1} g(s_1, s_2)ds_1 ds_2.$$

Now let Λ be the two-dimensional Fourier Transform of h. We have

$$\begin{aligned}
\Lambda(u_1, u_2) &= \int_{-\infty}^{+\infty}\int_{-\infty}^{+\infty} e^{i(u_1 x_1 + u_2 x_2)}h(x_1, x_2)dx_1 dx_2 \\
&= \int_{-\infty}^{+\infty}\int_{-\infty}^{+\infty} e^{i(u_1 x_1 + u_2 x_2)}\left(e^{-(a_1 x_1 + a_2 x_2)}\int_{-\infty}^{x_2}\int_{-\infty}^{x_1} g(s_1, s_2)ds_1 ds_2\right)dx_1 dx_2 \\
&= \int_{-\infty}^{+\infty}\int_{-\infty}^{+\infty}\int_{-\infty}^{x_2}\int_{-\infty}^{x_1} e^{i(u_1 x_1 + u_2 x_2)}e^{-(a_1 x_1 + a_2 x_2)}g(s_1, s_2)ds_1 ds_2 dx_1 dx_2.
\end{aligned}$$

Noting that $-\infty < s_1 < x_1 < +\infty$ and $-\infty < s_2 < x_2 < +\infty$, the expression of Λ becomes

$$\begin{aligned}\Lambda(u_1,u_2) &= \int_{-\infty}^{+\infty}\int_{-\infty}^{+\infty}\int_{s_2}^{+\infty}\int_{s_1}^{+\infty} e^{i(u_1x_1+u_2x_2)}e^{-(a_1x_1+a_2x_2)}g(s_1,s_2)dx_1dx_2ds_1ds_2 \\ &= \int_{-\infty}^{+\infty}\int_{-\infty}^{+\infty} g(s_1,s_2)\left(\int_{s_2}^{+\infty}\int_{s_1}^{+\infty} e^{i(u_1x_1+u_2x_2)}e^{-(a_1x_1+a_2x_2)}dx_1dx_2\right)ds_1ds_2.\end{aligned}$$

The double integral between parentheses can be computed as

$$\int_{s_2}^{+\infty}\int_{s_1}^{+\infty} e^{i(u_1x_1+u_2x_2)}e^{-(a_1x_1+a_2x_2)}dx_1dx_2 = \left[\frac{e^{-(a_1-iu_1)x_1}}{-(a_1-iu_1)}\right]_{s_1}^{+\infty}\left[\frac{e^{-(a_2-iu_2)x_2}}{-(a_2-iu_2)}\right]_{s_2}^{+\infty}.$$

Note that $\left|e^{-(a_1-iu_1)x_1}\right| \longrightarrow 0$ when x_1 goes to $+\infty$ and $\left|e^{-(a_2-iu_2)x_2}\right| \longrightarrow 0$ when x_2 goes to $+\infty$, so that we obtain

$$\begin{aligned}\Lambda(u_1,u_2) &= \int_{-\infty}^{+\infty}\int_{-\infty}^{+\infty} g(s_1,s_2)\left(-\frac{e^{-(a_1-iu_1)s_1}}{-(a_1-iu_1)}\right)\left(-\frac{e^{-(a_2-iu_2)s_2}}{-(a_2-iu_2)}\right)ds_1ds_2 \\ &= \frac{1}{(a_1-iu_1)(a_2-iu_2)}\int_{-\infty}^{+\infty}\int_{-\infty}^{+\infty} g(s_1,s_2)e^{i((u_1+ia_1)s_1+(u_2+ia_2)s_2)}ds_1ds_2 \\ &= \frac{\phi(u_1+ia_1,u_2+ia_2)}{(a_1-iu_1)(a_2-iu_2)}.\end{aligned}$$

The function h can be written as the two-dimensional inverse Fourier Transform of Λ:

$$h(x_1,x_2) = \frac{1}{4\pi^2}\int_{-\infty}^{+\infty}\int_{-\infty}^{+\infty} e^{-i(u_1x_1+u_2x_2)}\frac{\phi(u_1+ia_1,u_2+ia_2)}{(a_1-iu_1)(a_2-iu_2)}du_1du_2,$$

and G is then easily obtained as

$$G(x_1,x_2) = \frac{e^{a_1x_1+a_2x_2}}{4\pi^2}\int_{-\infty}^{+\infty}\int_{-\infty}^{+\infty} e^{-i(u_1x_1+u_2x_2)}\frac{\phi(u_1+ia_1,u_2+ia_2)}{(a_1-iu_1)(a_2-iu_2)}du_1du_2,$$

which concludes the proof. □

Proof. (Proposition 5)

Sklar's Theorem allows one to write the copula function of a pair of random variables from its joint distribution function as, for $(v_1,v_2)\in[0,1]^2$,

$$C(v_1,v_2,T) = G\left(G_1^{-1}(v_1,T),G_2^{-1}(v_2,T),T\right).$$

The expression for the copula function in Proposition 5 follows by using Lemma 4, which expresses the joint distribution function in terms of the joint characteristic function ϕ. Assuming $C(.,T)$ is absolutely continuous, we can write its copula density, for $(v_1,v_2)\in[0,1]^2$, as

$$c(v_1,v_2,T) = \frac{g(G_1^{-1}(v_1,T),G_2^{-1}(v_2,T),T)}{g_1(G_1^{-1}(v_1,T),T)g_2(G_2^{-1}(v_2,T),T)}.$$

Again, the expression for the copula density in Proposition 5 follows by using expressions (22), (23) and (24) that express the joint and marginal densities of $(X_1(T),X_2(T))$ in terms of the joint characteristic function ϕ. □

Acknowledgements

We thank Iain Clark, Jean-Baptiste Gheeraert, Cassio Neri, Damien Pons, Matthias Scherer, and seminar participants at the 53rd Meeting of the Euro Working Group on Commodities and Financial Modelling, the International Ruhr Energy Conference 2015, and the World Finance Conference 2015 for helpful and stimulating comments, discussions and suggestions. All remaining errors are our own.

Appendix A. Kummer's functions

The functions M and U are the confluent hypergeometric functions. The function M is also known as ${}_1F_1$, and the function U as Tricomi's function. Given, $a, b, z \in \mathbb{C}$, Kummer's equation is

$$z\frac{\partial^2 w}{\partial z^2} + (b - z)\frac{\partial w}{\partial z} - aw = 0. \tag{A.1}$$

A way to obtain $M(a, b, z)$ is by means of the series expansion

$$M(a, b, z) = 1 + \sum_{n=1}^{\infty} \frac{z^n \prod_{j=1}^{n} (a + j - 1)}{n! \prod_{j=1}^{n} (b + j - 1)}. \tag{A.2}$$

And $U(a, b, z)$ is obtained from M as

$$U(a, b, z) = \frac{\pi}{\sin(\pi b)} \left(\frac{M(a, b, z)}{\Gamma(1 + a - b)\Gamma(b)} - z^{1-b} \frac{M(1 + a - b, 2 - b, z)}{\Gamma(a)\Gamma(2 - b)} \right), \tag{A.3}$$

where Γ denotes the Gamma function extended to the complex plane. These results and additional properties of Kummer's functions (e.g. integral representations) can be found in Chap. 13 of Abramovitz and Stegun (1972). A detailed analysis of how to implement Kummer's functions is given by Pearson (2009). A suitable way to implement the complex Gamma function is the Lanczos (1964) approximation.

Appendix B. The Caldana and Fusai method for pricing calendar spread options.

Let $\Phi_T(u) = \Phi(u)$ be the joint characteristic function of the logarithms $\ln F(T, T_1), \ln F(T, T_2)$ of two futures prices as given in the main manuscript. Following Caldana and Fusai (2013), the price of the calendar spread option call with maturity T and strike K is given in terms of a Fourier inversion formula as

$$CSC(0, K, T, T_1, T_2) = \left(\frac{e^{-\delta k - rT}}{\pi} \int_0^{+\infty} e^{-i\gamma k} \Psi_T(\gamma; \delta, \alpha) d\gamma \right)^+, \tag{B.1}$$

where

$$\Psi_T(\gamma; \delta, \alpha) = \frac{e^{i(\gamma - i\delta)\ln(\Phi_T(0, -i\alpha))}}{i(\gamma - i\delta)} \cdot \left[\Phi_T\left((\gamma - i\delta) - i, -\alpha(\gamma - i\delta)\right) - \Phi_T\left(\gamma - i\delta, -\alpha(\gamma - i\delta) - i\right) - K\Phi_T\left(\gamma - i\delta, -\alpha(\gamma - i\delta)\right) \right]$$

and

$$\alpha = \frac{F(0, T_2)}{F(0, T_2) + K}, \qquad k = \ln(F(0, T_2) + K).$$

The parameter δ controls an exponential decay term as in Carr and Madan (1999).

Appendix C. FFT Methods

An FFT algorithm allows the efficient computation of Discrete Fourier Transforms (DFT) of vectors and matrices. Here we will discuss Matlab and Numerical Recipes in C++ functions but other numerical analysis tools, such as Mathematica and R, are of course also suitable.

Matlab functions:

In one dimension, the Matlab routines `fft` and `ifft` work with vectors and implement the following sums, respectively:

$$x(k) = \sum_{n=1}^{N} X(n) W_N^{(n-1)(k-1)} \qquad X(n) = \frac{1}{N} \sum_{k=1}^{N} x(k) W_N^{-(n-1)(k-1)} \tag{C.1}$$

where $W_N = e^{\frac{-2\pi i}{N}}$ is a Nth root of unity.

In two dimensions, the Matlab routines `fft2` and `ifft2` work with matrices and implement the following sums, respectively:

$$x(k_1, k_2) = \sum_{n_1=1}^{N} \sum_{n_2=1}^{N} X(n_1, n_2) W_N^{[(n_1-1)(k_1-1)+(n_2-1)(k_2-1)]} \tag{C.2}$$

$$X(n_1, n_2) = \frac{1}{N^2} \sum_{k_1=1}^{N} \sum_{k_2=1}^{N} x(k_1, k_2) W_N^{-[(n_1-1)(k_1-1)+(n_2-1)(k_2-1)]} \tag{C.3}$$

where $W_N = e^{\frac{-2\pi i}{N}}$ is an Nth root of unity.

Numerical Recipes in C++ functions:

In one dimension, the function `four1` works with vectors and implements the following sums when choosing `isign` $= 1$ and -1, respectively:

$$H(n) = \sum_{k=0}^{N-1} h(k) W_N^{nk} \qquad h(k) = \sum_{n=0}^{N-1} H(n) W_N^{-nk} \tag{C.4}$$

where $W_N = e^{\frac{2\pi i}{N}}$ is a Nth root of unity.

In two dimensions, the function `fourn` works with matrices and implements the following sums when choosing `isign` $= 1$ and -1, respectively:

$$H(n_1, n_2) = \sum_{k_1=0}^{N-1} \sum_{k_2=0}^{N-1} h(k_1, k_2) W_N^{n_1 k_1 + n_2 k_2} \tag{C.5}$$

$$h(k_1, k_2) = \sum_{n_1=0}^{N-1} \sum_{n_2=0}^{N-1} H(n_1, n_2) W_N^{-(n_1 k_1 + n_2 k_2)} \tag{C.6}$$

where $W_N = e^{\frac{2\pi i}{N}}$ is an Nth root of unity (note that W_N is not the same as in Matlab).

Appendix D. Marginal CDF and PDF

We are first interested in the marginal CDF and PDF of $X_1(T)$.

Let N be the chosen number of points on the grid (e.g. $N = 512$) and let $x_{k_1} = \left(k_1 - \frac{N}{2}\right) h$ with $k_1 = 0, \ldots, N-1$. h is the chosen distance between points in the initial domain. The grid in x is centered on $x_{\frac{N}{2}} = 0$. In the transformed domain we work with $\omega = \frac{u}{2\pi}$ that represents angular frequency (u represents frequency or inverse wavelength). N is also the chosen number of points on the grid in ω with $\omega_{n_1} = \left(n_1 - \frac{N}{2}\right) s$ with $n_1 = 0, \ldots, N-1$. $s = \frac{1}{hN}$ is the distance between points in the transformed domain. The grid in the transformed domain is centered on $\omega_{\frac{N}{2}} = 0$.

At a point x_{k_1}, choosing the rectangle rule on the grid in ω, the PDF g_1 is approximated as

$$g_1(x_{k_1}, T) = \int_{-\infty}^{+\infty} e^{-i2\pi\omega\left(k_1 - \frac{N}{2}\right)h} \phi(2\pi\omega, 0, T) d\omega \approx s \sum_{n_1=0}^{N-1} e^{-i2\pi\left(n_1 - \frac{N}{2}\right)\left(k_1 - \frac{N}{2}\right)sh} \phi(2\pi\omega_{n_1}, 0, T) \tag{D.1}$$

$$\approx s(-1)^{k_1 - \frac{N}{2}} \sum_{n_1=0}^{N-1} (-1)^{n_1} \phi(2\pi\omega_{n_1}, 0, T) e^{n_1 k_1 \frac{-i2\pi}{N}} \tag{D.2}$$

where the powers of -1 appear when rearranging terms and noting that $e^{iq\pi} = (-1)^q$ for $q \in \mathbb{Z}$. When N is a power of 2, the obtained expression is suitable for FFT algorithms at hand. For $x_0, \ldots, x_{N-1}$, the sums can be computed by calling just once the FFT function on the vector

$$\left[(-1)^n \phi(2\pi\omega_{n_1}), n_1 = 0, \ldots, N-1\right].$$

In Matlab it corresponds to the `fft` routine and in Numerical Recipes to the function `four1` with `isign`$= -1$. Other approximations can be obtained using different numerical integration rules (e.g. trapezoidal, Simpson).

With the same grids and notations, at a point x_{k_1}, the CDF G_1 is written, with $a > 0$,

$$G_1(x_{k_1}, T) = \frac{1}{2} - \frac{1}{2\pi} \int_{-\infty}^{+\infty} e^{-iux_{k_1}} \frac{\phi(u)}{iu} du = \frac{e^{ax_{k_1}}}{2\pi} \int_{-\infty}^{+\infty} e^{-iux_{k_1}} \frac{\phi(u + ia, 0, T)}{a - iu} du. \tag{D.3}$$

A proper choice for the value of a (e.g. $a = 3$) will permit a smoothing of the singularity at $u = 0$ of the integrand in the initial CDF inversion result. At a point x_{k_1}, choosing the rectangle rule on the grid in ω, the CDF G_1 can now be approximated as

$$G_1(x_{k_1}, T) \approx e^{ax_{k_1}} s \sum_{n_1=0}^{N-1} \frac{\phi(2\pi\omega_{n_1} + ia, 0, T)}{a - i2\pi\omega_{n_1}} e^{-i2\pi\left(n_1 - \frac{N}{2}\right)\left(k_1 - \frac{N}{2}\right)sh}, \tag{D.4}$$

$$\approx e^{ax_{k_1}} s(-1)^{k_1 - \frac{N}{2}} \sum_{n_1=0}^{N-1} (-1)^{n_1} \frac{\phi(2\pi\omega_{n_1} + ia, 0, T)}{a - i2\pi\omega_{n_1}} e^{n_1 k \frac{-i2\pi}{N}}. \tag{D.5}$$

The powers of -1 appear once again for the reason already mentioned. With N a power of 2, the obtained expression is suitable for FFT algorithms and the needed sums on the x-grid are computed by calling just once the FFT function on the vector

$$\left[(-1)^{n_1} \frac{\phi(2\pi\omega_{n_1} + ia)}{a - i2\pi\omega_{n_1}}, n_1 = 0, \ldots, N-1\right].$$

In Matlab it corresponds to the `fft` routine and in Numerical Recipes to the function `four1` with `isign`$= -1$.

Once G_1 has been implemented, it is rather easy to implement the inverse CDF G_1^{-1} either with a numerical root search or by doing a reverse interpolation on the pair of vectors

$$\left([x_0, \ldots, x_{N-1}], [G_1(x_0), \ldots, G_1(x_{N-1})]\right).$$

Appendix E. Joint CDF and PDF

Let N be again the chosen number of points on the one-dimensional grids in x_1 and x_2 (e.g. $N = 512$) and let $x_{k_1} = \left(k_1 - \frac{N}{2}\right) h$ and $x_{k_2} = \left(k_2 - \frac{N}{2}\right) h$ with $k_1, k_2 = 0, \ldots, N-1$. h is the chosen distance between points in the initial domain. The grid is centered on $\left(x_{\frac{N}{2}}, x_{\frac{N}{2}}\right) = (0,0)$. In the transformed domain we work with $\upsilon = \frac{u_1}{2\pi}$ and $\omega = \frac{u_2}{2\pi}$. N is also the chosen number of points on the one-dimensional grids in υ and ω with $\upsilon_{n_1} = \left(n_1 - \frac{N}{2}\right) s$ and $\omega_{n_2} = \left(n_2 - \frac{N}{2}\right) s$ with $n_1, n_2 = 0, \ldots, N-1$. $s = \frac{1}{hN}$ is the distance between points in the transformed domain. The grid in the transformed domain is centered on $\left(\upsilon_{\frac{N}{2}}, \omega_{\frac{N}{2}}\right) = (0,0)$. At a point (x_{k_1}, x_{k_2}), choosing the two-dimensional rectangle rule on the grid in (υ, ω), the joint PDF g is approximated as

$$g(x_{k_1}, x_{k_2}, T) = \int_{-\infty}^{+\infty} \int_{-\infty}^{+\infty} e^{-i2\pi(\upsilon x_{k_1} + \omega x_{k_2})} \phi(2\pi\upsilon, 2\pi\omega, T) d\upsilon d\omega, \tag{E.1}$$

$$\approx s^2 \sum_{n_1=0}^{N-1} \sum_{n_2=0}^{N-1} \phi(2\pi\upsilon_{n_1}, 2\pi\omega_{n_2}, T) e^{-i2\pi\left[\left(n_1 - \frac{N}{2}\right)\left(k_1 - \frac{N}{2}\right) + \left(n_2 - \frac{N}{2}\right)\left(k_2 - \frac{N}{2}\right)\right] sh}, \tag{E.2}$$

$$\approx s^2 (-1)^{k_1 + k_2 - N} \sum_{n_1=0}^{N-1} \sum_{n_2=0}^{N-1} (-1)^{n_1+n_2} \phi(2\pi\upsilon_{n_1}, 2\pi\omega_{n_2}, T) e^{(n_1 k_1 + n_2 k_2)\frac{-i2\pi}{N}}. \tag{E.3}$$

With N a power of 2, the obtained expression is suitable for FFT algorithms in 2D and the needed sums on the (x_1, x_2)-grid are computed by calling just once the FFT function on the matrix

$$[(-1)^{n_1, n_2} \phi(2\pi\upsilon_{n_1}, 2\pi\omega_{n_2}, T), n_1, n_2 = 0, \ldots, N-1]$$

In Matlab it corresponds to the `fft2` routine and in Numerical Recipes to the function `fourn` with `isign`$=$ -1.

With the same grids and notations, at a point (x_{k_1}, x_{k_2}), the joint CDF G can be written, with $a_1, a_2 > 0$,

$$G(x_{k_1}, x_{k_2}, T) = \frac{e^{a_1 x_{k_1} + a_2 x_{k_2}}}{4\pi^2} \int_{-\infty}^{+\infty} \int_{-\infty}^{+\infty} e^{-i(u_1 x_{k_1} + u_2 x_{k_2})} \frac{\phi(u_1 + ia_1, u_2 + ia_2, T)}{(a_1 - iu_1)(a_2 - iu_2)} du_1 du_2 \tag{E.4}$$

Here again, a proper choice for the value of a_1 and a_2 (e.g. $a_1 = a_2 = 3$) will permit a smoothing of the singularity of the integrand on the axis $u_1 = 0$ and $u_2 = 0$ in the initial joint CDF inversion result.

At a point (x_{k_1}, x_{k_2}), choosing the two-dimensional rectangle rule on the grid in (υ, ω), the joint CDF G is approximated as

$$G(x_{k_1}, x_{k_2}, T) = e^{a_1 x_{k_1} + a_2 x_{k_2}} \int_{-\infty}^{+\infty} \int_{-\infty}^{+\infty} e^{-i2\pi(\upsilon x_{k_1} + \omega x_{k_2})} \frac{\phi(2\pi\upsilon + ia_1, 2\pi\omega + ia_2, T)}{(a_1 - i2\pi\upsilon)(a_2 - i2\pi\omega)} d\upsilon d\omega, \tag{E.5}$$

$$\approx e^{a_1 x_{k_1} + a_2 x_{k_2}} s^2 \sum_{n_1=0}^{N-1} \sum_{n_2=0}^{N-1} \frac{\phi(2\pi\upsilon_{n_1} + ia_1, 2\pi\omega_{n_2} + ia_2, T)}{(a_1 - i2\pi\upsilon_{n_1})(a_2 - i2\pi\omega_{n_2})} e^{-i2\pi[(n_1 - \frac{N}{2})(k_1 - \frac{N}{2}) + (n_2 - \frac{N}{2})(k_2 - \frac{N}{2})]sh}, \tag{E.6}$$

$$\approx e^{a_1 x_{k_1} + a_2 x_{k_2}} s^2 (-1)^{k_1 + k_2 - N} \sum_{n_1=0}^{N-1} \sum_{n_2=0}^{N-1} (-1)^{n_1 + n_2} \frac{\phi(2\pi\upsilon_{n_1} + ia_1, 2\pi\omega_{n_2} + ia_2, T)}{(a_1 - i2\pi\upsilon_{n_1})(a_2 - i2\pi\omega_{n_2})} e^{(n_1 k_1 + n_2 k_2)\frac{-i2\pi}{N}}. \tag{E.7}$$

With N a power of 2, the obtained expression is suitable for FFT algorithms in 2D and the needed sums on the (x_1, x_2)-grid are computed by calling just once the FFT function on the matrix

$$\left[(-1)^{n_1, n_2} \frac{\phi(2\pi\upsilon_{n_1} + ia_1, 2\pi\omega_{n_2} + ia_2, T)}{(a_1 - i2\pi\upsilon_{n_1})(a_2 - i2\pi\omega_{n_2})}, n_1, n_2 = 0, \ldots, N-1 \right]$$

In Matlab it corresponds to the `fft2` routine and in Numerical Recipes to the function `fourn` with `isign`= -1.

References

Abramovitz, M., Stegun, I. A., 1972. Handbook of mathematical functions, tenth printing Edition. Applied Mathematics Series 55. National Bureau of Standards.

Bakshi, G., Cao, C., Chen, Z., December 1997. Empirical performance of alternative option pricing models. Journal of Finance 52 (5), 2003–2049.

Bakshi, G., Madan, D., 2000. Spanning and derivative-security valuation. Journal of Financial Economics 55 (2), 205–238.

Barone-Adesi, G., Whaley, R. E., June 1987. Efficient analytic approximation of American option values. Journal of Finance 42 (2), 301–320.

Bessembinder, H., Coughenour, J. F., Seguin, P. J., Smoller, M. M., Winter 1996. Is there a term structure of futures volatilities? Reevaluating the Samuelson hypothesis. Journal of Derivatives 4 (2), 45–58.

Bjerksund, P., Stensland, G., 2011. Closed form spread option valuation. Quantitative Finance iFirst, 1–10.

Black, F., March 1976. The pricing of commodity contracts. Journal of Financial Economics 3 (1-2), 167–179.

Brooks, R., Winter 2012. Samuelson hypothesis and carry arbitrage. Journal of Derivatives 20 (2), 37–65.

Caldana, R., Fusai, G., December 2013. A general closed-form spread option pricing formula. Journal of Banking and Finance 37 (12), 4893–4906.

Carmona, R., Durrleman, V., 2003. Pricing and hedging spread options. SIAM Review 45 (4), 627–685.

Carr, P., Madan, D. B., 1999. Option valuation using the Fast Fourier Transform. Journal of Computational Finance 2 (4), 61–73.

Chockalingam, A., Muthuraman, K., July–August 2011. American options under stochastic volatility. Operations Research 59 (4), 793–809.

Christoffersen, P., Heston, S., Jacobs, K., December 2009. The shape and term structure of the index option smirk: Why multifactor stochastic volatility models work so well. Management Science 55 (12), 1914–1932.

Clark, I. J., 2014. Commodity Option Pricing: A Practitioner's Guide. Wiley Finance. Wiley.

Clewlow, L., Strickland, C., August 1999a. A multi-factor model for energy derivatives, working Paper, 20 pages.

Clewlow, L., Strickland, C., April 1999b. Valuing energy options in a one factor model fitted to forward prices, working Paper, 30 pages.

Cox, J. C., Ingersoll, J. E., Ross, S. A., 1985. A theory of the term structure of interest rates. Econometrica 53, 385–408.

Duffie, D., Pan, J., Singleton, K., November 2000. Transform analysis and asset pricing for affine jump-diffusions. Econometrica 68 (6), 1343–1376.

Heston, S., 1993. A closed-form solution for options with stochastic volatility with applications to bond and currency options. Review of Financial Studies 6 (2), 327–343.

Hull, J., White, A., June 1987. The pricing of options on assets with stochastic volatilities. Journal of Finance 42 (2), 281–100.

Hurd, T. R., Zhou, Z., 2010. A Fourier transform method for spread option pricing. SIAM Journal on Financial Mathematics 1 (1), 142–157.

Kirk, E., 1995. Correlations in the energy markets. Managing Energy Price Risk, 71–78.

Lanczos, C., 1964. A precision approximation of the Gamma function. SIAM Journal on Numerical Analysis series B 1, 86–96.

Le Courtois, O., Walter, C., 2015. The computation of risk budgets under the Lévy process assumption. Finance 35 (2).

Longstaff, F. A., Schwartz, E. S., 2001. Valuing American options by simulation: A simple least-squares approach. Review of Financial Studies 14 (1), 113–147.

Mai, J.-F., Scherer, M., 2012. Simulating Copulas: Stochastic Models, Sampling Algorithms, and Applications. Vol. 4 of Series in Quantitative Finance. Imperial College Press.

Margrabe, W., March 1978. The value of an option to exchange one asset for another. Journal of Finance 33 (1), 177–186.

Nelsen, R. B., 2006. An Introduction to Copulas, 2nd Edition. Springer Series in Statistics. Springer.

Øksendal, B., 2003. Stochastic Differential Equations: An Introduction with Applications, sixth Edition. Universitext. Springer.

Pearson, J., September 2009. Computation of hypergeometric functions. Master's thesis, University of Oxford.

Samuelson, P. A., Spring 1965. Proof that properly anticipated prices fluctuate randomly. Industrial Management Review 6 (2), 41–49.

Schoebel, R., Zhu, J., 1999. Stochastic volatility with an Ornstein-Uhlenbeck process: An extension. European Finance Review 3, 23–46.

Scott, L. O., December 1987. Option pricing when the variance changes randomly: Theory, estimation, and an application. Journal of Financial and Quantitative Analysis 22 (4), 419–438.

Scott, L. O., October 1997. Pricing stock options in a jump-diffusion model with stochastic volatility and interest rates: Applications of Fourier inversion methods. Mathematical Finance 7 (4), 413–424.

Trolle, A. B., Schwartz, E. S., 2009. Unspanned stochastic volatility and the pricing of commodity derivatives. Review of Financial Studies 22 (11), 4423–4461.

Venkatramanan, A., Alexander, C., November 2011. Closed-form approximations for spread options. Applied Mathematical Finance 18 (5), 447–472.